

Pressure suppression of the excitonic insulator state in Ta₂NiSe₅ observed by optical conductivity

H. Okamura,* T. Mizokawa¹, K. Miki, Y. Matsui, N. Noguchi, N. Katayama²,
H. Sawa², M. Nohara³, Y. Lu⁴, H. Takagi^{5,6}, Y. Ikemoto⁷, and T. Moriwaki⁷

Department of Applied Chemistry, Tokushima University, Tokushima 770-8506, Japan

¹*Department of Applied Physics, Waseda University, Tokyo 169-8555, Japan*

²*Department of Applied Physics, Nagoya University, Nagoya 464-8603, Japan*

³*Department of Quantum Matter, Hiroshima University, Higashi-Hiroshima 739-8503, Japan*

⁴*College of Materials Science and Engineering, National Engineering Research Center for Magnesium Alloys, Chongqing University, Chongqing 400044, China*

⁵*Department of Physics, University of Tokyo, Tokyo 113-0013, Japan*

⁶*Max Planck Institute for Solid State Research, 70569 Stuttgart, Germany and*

⁷*Japan Synchrotron Radiation Research Institute, Sayo 679-5198, Japan*

(Dated: August 26, 2022)

The layered chalcogenide Ta₂NiSe₅ has recently attracted much interest as a strong candidate for the long sought excitonic insulator (EI). Since the physical properties of an EI are expected to depend sensitively on the external pressure, it is important to clarify the pressure evolution of microscopic electronic state in Ta₂NiSe₅. Here we report the optical conductivity [$\sigma(\omega)$] of Ta₂NiSe₅ measured at high pressures to 10 GPa and at low temperatures to 8 K. With cooling at ambient pressure, $\sigma(\omega)$ develops an energy gap of about 0.17 eV and a pronounced excitonic peak at 0.38 eV, as already reported in the literature. Upon increasing pressure, the energy gap becomes narrower and the excitonic peak is broadened. Above a structural transition at $P_s \simeq 3$ GPa, the energy gap becomes partially filled, indicating that Ta₂NiSe₅ is a semimetal after the EI state is suppressed by pressure. At higher pressures, $\sigma(\omega)$ exhibits metallic characteristics with no energy gap. The detailed pressure evolution of $\sigma(\omega)$ is presented, and discussed mainly in terms of a weakening of excitonic correlation with pressure.

I. INTRODUCTION

Excitonic insulator (EI) is an unconventional insulator in which the attractive correlation between electrons and holes results in a collective condensation of electron-hole (e - h) pairs (excitons) and an energy gap at the Fermi level (E_F). EI was first predicted theoretically in the 1960s,¹ with a phase diagram schematically shown in Fig. 1. The starting material for EI can be either semimetal ($E_g < 0$) or semiconductor ($E_g > 0$), where E_g indicates the one-particle band gap in the absence of e - h correlation. An EI state is expected in the vicinity of $E_g=0$ below the transition temperature T_c if the exciton binding energy E_b is larger than $|E_g|$. Another feature of the EI is a characteristic flattening of the bands indicated in Fig. 1.

Despite the theoretical interest on EI, only a few compounds had been considered as candidates for EI, including TmSe_{1-x}Te_x² and 1T-TiSe₂.³ In 2009, Wakisaka *al.*⁴ suggested that Ta₂NiSe₅ should be an EI on the basis of angle-resolved photoemission spectroscopy (ARPES) data. Ta₂NiSe₅ has a layered crystal structure, and exhibits a structural phase transition at $T_c=328$ K, where the crystal symmetry changes from orthorhombic to monoclinic with decreasing temperature (T).^{5,6} Below T_c , the resistivity increases rapidly with cooling, indicating an energy gap of about 0.2 eV.⁶ The ARPES study at 10 K found an unusually flat dispersion at the top of the valence band, which was regarded as strong evidence for an EI. Further ARPES study⁷ and band calculation^{7,8} indicate

that the flat band feature persisted even above T_c , and suggested the low- T phase of Ta₂NiSe₅ to be an EI in the strong coupling regime caused by a condensation of preformed excitons.^{7,8} It was pointed out that above T_c

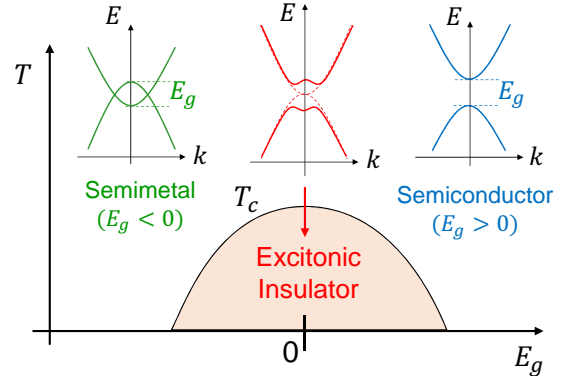


FIG. 1: Schematic phase diagram of EI in terms of the temperature (T) and the one-particle band gap in the absence of e - h correlation (E_g). Positive and negative values of E_g correspond to semiconducting and semimetallic states, respectively. An EI state is expected in the vicinity of $E_g=0$ below the transition temperature (T_c), with a characteristic flattening of the band edges as indicated.

by symmetry. It was also suggested that the structural change below T_c was mainly driven by the exciton condensation, rather than by a structural instability due to electron-lattice ($e-l$) coupling.⁸ Lu et al⁹ reported transport and optical data of $\text{Ta}_2\text{Ni}(\text{Se},\text{S})_5$ and $\text{Ta}_2\text{Ni}(\text{Se},\text{Te})_5$ where the chemical substitution and external pressure were used to control E_g of Ta_2NiSe_5 . The optical conductivity $[\sigma(\omega)]$ of Ta_2NiSe_5 at low T clearly exhibited a pronounced peak of excitonic origin at about 0.4 eV, and an energy gap of about 0.16 eV. An experimental phase diagram of Ta_2NiSe_5 was constructed from the transport data, which was indeed consistent with the predicted one depicted in Fig. 1 and strongly suggested Ta_2NiSe_5 to be an EI.⁹ Detailed $\sigma(\omega)$ data¹⁰ were analyzed by a theoretical study,¹¹ which again suggested that Ta_2NiSe_5 should be an EI in the strong coupling regime below T_c , and it should be a semiconductor ($E_g > 0$) above T_c .¹¹

Many more works on Ta_2NiSe_5 have also been reported, including ARPES,^{12–21} optical conductivity,^{22,23} Raman scattering,^{24–28} ultrafast laser spectroscopy,^{29–31} resonant inelastic X-ray scattering,^{32,33} high pressure studies,^{23,26,34} scanning tunneling spectroscopy,³⁵ and theoretical analyses.^{20,36,37} While many of these works support that the transition at T_c is driven by exciton condensation, some of them question such scenario.^{20,33,36} For example, a semimetallic ($E_g < 0$) band dispersion around E_F has been reported by an ARPES study above T_c .²⁰ Theoretically, it has been shown that a flat valence band may be obtained by a band calculation without $e-l$ correlation,²⁰ and that there can be a sizable (~ 0.1 eV) hybridization with the mirror symmetry breaking below T_c but without $e-h$ correlation.³⁶

Following the above development, it is important to carefully evaluate effects of both the $e-h$ correlation and $e-l$ coupling in Ta_2NiSe_5 . An important aspect is the response of Ta_2NiSe_5 to changes in the ratio E_b/E_g , since the physical properties of EI should sensitively depend on E_b/E_g . In this regard, photo-excited experiments, which are probed by either ARPES^{12–17} or laser,^{29–31} have the advantage of being able to tune the carrier density, and hence to control E_b through the Coulomb screening of $e-h$ attraction. In fact, photo-induced gap closing and semimetallic states in Ta_2NiSe_5 have been observed and analyzed.^{12–17,31} Another effective way of tuning an EI state is the application of external pressure (P),^{9,23,26,34} since an applied pressure usually broadens the conduction and valence bands, and increases (reduces) their overlap (separation). Detailed high- P studies^{23,34} have been performed on the crystal structure, resistivity (ρ), Hall coefficient, and $\sigma(\omega)$ of Ta_2NiSe_5 . They revealed a rich P - T phase diagram of Ta_2NiSe_5 as depicted in Fig. 2. Above the first order structural transition at $P_s \simeq 3$ GPa, the ac plane becomes flatter with a less rippling of ac plane along the c axis.^{23,34} $\rho(T)$ is reduced with increasing P , showing a crossover from semiconducting T dependence below P_s to a completely metallic one well above P_s , with quite large and dramatic change of $\rho(T)$ around P_s . A superconductivity with $T_c=2$ K appears at

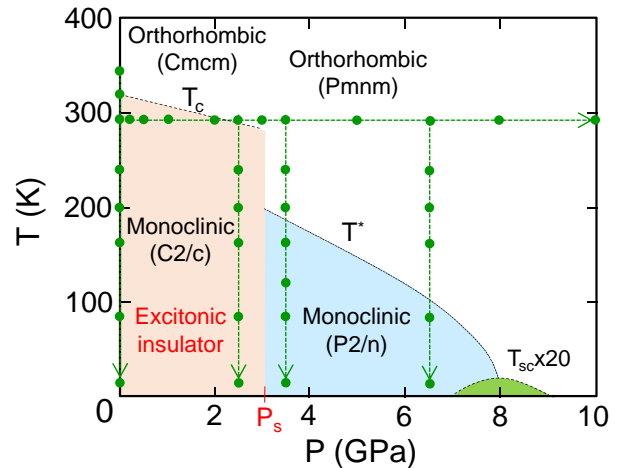


FIG. 2: Temperature (T)-pressure (P) phase diagram of Ta_2NiSe_5 reproduced from Matsubayashi *et al.*²³ T_c , T^* , and P_s indicate the structural transition temperatures and pressure, and T_{sc} the superconducting transition temperature. The green arrows and dots indicate the (P, T) paths and points where $\sigma(\omega)$ was measured in this work.

about 8 GPa. Above P_s , from $\rho(T)$ and $\sigma(\omega)$ data, it has been shown that Ta_2NiSe_5 is a semimetal with a partial energy gap, in contrast to the full energy gap below P_s . It has been suggested that the electronic transition at T^* to the low- T semimetallic state is caused by $e-l$ coupling, while that at T_c below P_s is caused by both excitonic correlation and $e-l$ coupling.²³

In this paper, we present a full account of the $\sigma(\omega)$ and reflectance data of Ta_2NiSe_5 at high P and low T , which have been obtained at the (P, T) points indicated in Fig. 2. The data reveal how the well-developed energy gap and excitonic peak at $P=0$, which have been taken as evidence for an EI, are suppressed as the applied pressure reduces the excitonic correlation.

II. EXPERIMENTAL

The samples of Ta_2NiSe_5 used were single crystals grown with the chemical vapor transport method as reported previously.⁹ The reflectance spectrum at zero external pressure [$R_0(\omega)$] was measured at 0.015–4.5 eV photon energy range³⁸ on an as-grown, specular surfaces. $\sigma(\omega)$ was derived from the measured $R_0(\omega)$ using the standard Kramers-Kronig (KK) analysis.³⁹ Below the measured energy range, $R_0(\omega)$ was extrapolated by the Hagen-Rubens function or a constant, depending on the data.³⁹ Above the measured range, it was extrapolated by a function of the form ω^{-d} .⁴⁰ T dependence of $R_0(\omega)$ were measured below 1.4 eV, and above 1.4 eV the $R_0(\omega)$ at 295 K was connected. Reflectance spectra at high P were measured using a diamond anvil cell (DAC).⁴¹ Type

IIa diamond anvils with a 0.8 mm culet diameter and a stainless steel gasket were used to seal the sample with KBr as the pressure transmitting medium. An as-grown surface of a sample was directly attached on the culet surface of the diamond anvil, and the reflectance at the sample/diamond interface [$R_d(\omega)$] was measured. A gold film was also sealed with the sample as the reference reflectance. The pressure in the DAC was measured with the ruby fluorescence method.⁴² $R_d(\omega)$ at high P and low T were measured at photon energies between 0.025 and 1.1 eV, using synchrotron radiation as a bright infrared source⁴⁴ at the beamline BL43IR of SPring-8.⁴⁵ The measured $R_d(\omega)$ spectra below 1.1 eV were connected to the $R_d(\omega)$ above 1.1 eV given by the KK analysis of measured $R_0(\omega)$ at 295 K and the refractive index of diamond ($n_d=2.4$). Then the connected $R_d(\omega)$ spectra were used to obtain $\sigma(\omega)$ by a modified KK analysis.⁴³ More details of the high pressure infrared experiments are reported elsewhere.⁴¹

III. RESULTS AND DISCUSSIONS

In the crystal structure of Ta_2NiSe_5 , the (-Ta-Se-) and (-Ni-Se-) chains extend along the a axis in the a - c layers stacked along the b axis.^{5,6} Therefore, characteristic optical responses of EI are expected with $E \parallel a$ polarization where E is the electric field of the incident light. $R_0(\omega)$ and $\sigma(\omega)$ spectra of Ta_2NiSe_5 measured at ambient pressure ($P=0$) are indicated in Figs. 3(a) and 3(b) respectively. In the $E \parallel a$ data, with cooling, $R_0(\omega)$ exhibits large T dependences. $\sigma(\omega)$ develops a clear energy gap with the onset at about 0.17 eV, as indicated by the broken line in Fig. 3(b), and a pronounced peak centered at $\simeq 0.38$ eV.⁴⁶ The sharp spikes below 0.05 eV are due to optical phonons and the periodic oscillations below 0.1 eV are due to interference caused by internal reflections from the rear surface of the sample. In contrast, in the $E \parallel c$ data, both $R_0(\omega)$ and $\sigma(\omega)$ are much lower than those in the $E \parallel a$ data, and their T dependence is much smaller. At 8 K, the onset of $\sigma(\omega)$ appears to be located around 0.3 eV, with only a gradual increase of $\sigma(\omega)$ above the onset. These results are very similar to previously reported $P=0$ data in the literature.^{9,10,22} The development of the energy gap and the pronounced peak with $E \parallel a$ have been interpreted as the result of EI state formation below T_c . The peak at 0.38 eV is an excitonic peak, as already discussed in Introduction, and its origin can be basically understood in terms of a band flattening as illustrated in Fig. 3(c). In a conventional insulator, the optical excitation between the band edges lead to the increase of $\sigma(\omega)$ above the band gap, as indicated by the green curves in Fig. 3(c). The spectrum in this case is actually similar to that measured with $E \parallel c$ in Fig. 3(b). In the case of EI, in contrast, the band edges are flattened by excitonic correlation. This results in a larger density of states (DOS) at the band edges, which should cause an enhancement in $\sigma(\omega)$ as shown by the

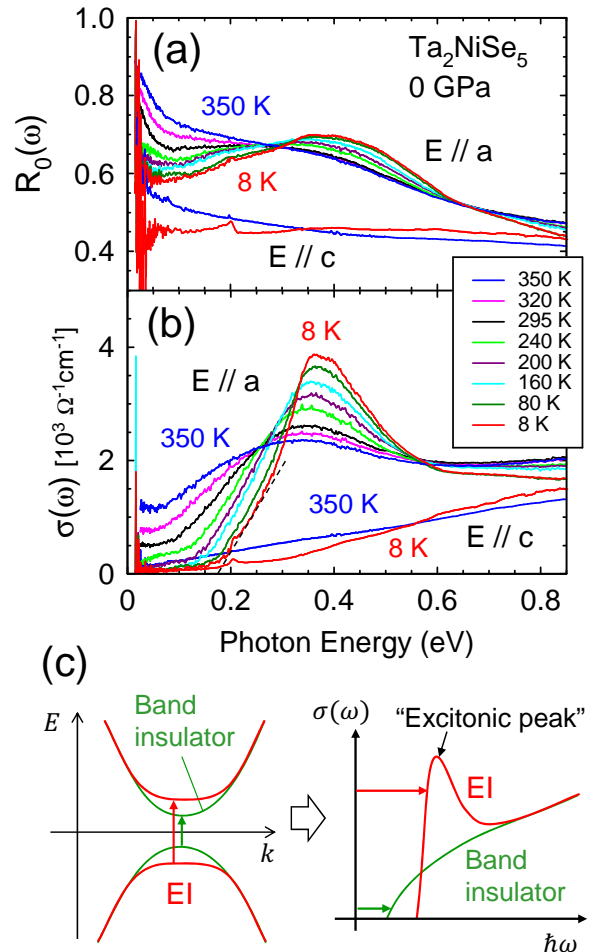


FIG. 3: (a) Optical reflectance [$R_0(\omega)$] and (b) conductivity [$\sigma(\omega)$] of Ta_2NiSe_5 at different temperatures and at ambient pressure. $E \parallel a$ and $E \parallel c$ denote incident light polarized along a and c axes, respectively. The broken line in (b) is a guide to the eye, indicating the onset at 0.17 eV. (c) Schematic diagrams indicating the optical transitions in an EI (red curves) and a band insulator (green curves).

red curves in Fig. 3(c). The spectrum in this case is very similar to that observed with $E \parallel a$ in Fig. 3(b). The T evolution of $\sigma(\omega)$ in Ta_2NiSe_5 has also been discussed in terms of exciton-phonon Fano effect¹⁰ and exciton superfluid formation.²² The shifts of the onset and the transfer of spectral weight in $\sigma(\omega)$ will be discussed later.

Pressure evolution of $R_d(\omega)$ and $\sigma(\omega)$ at 295 K with $E \parallel a$ is shown in Figs. 4(a)-4(c). Upon applying pressure, both $R_d(\omega)$ and $\sigma(\omega)$ below 0.2 eV exhibit large increases. In particular, $\sigma(\omega)$ below ~ 0.2 eV, which is reduced by the energy gap at $P=0$, rapidly increases with P . In addition, the excitonic peak is broadened and redshifted with P , and is almost suppressed at 3 GPa and above. This is more clearly seen in Fig. 4(c) where the spectra are vertically offset. The large spectral change

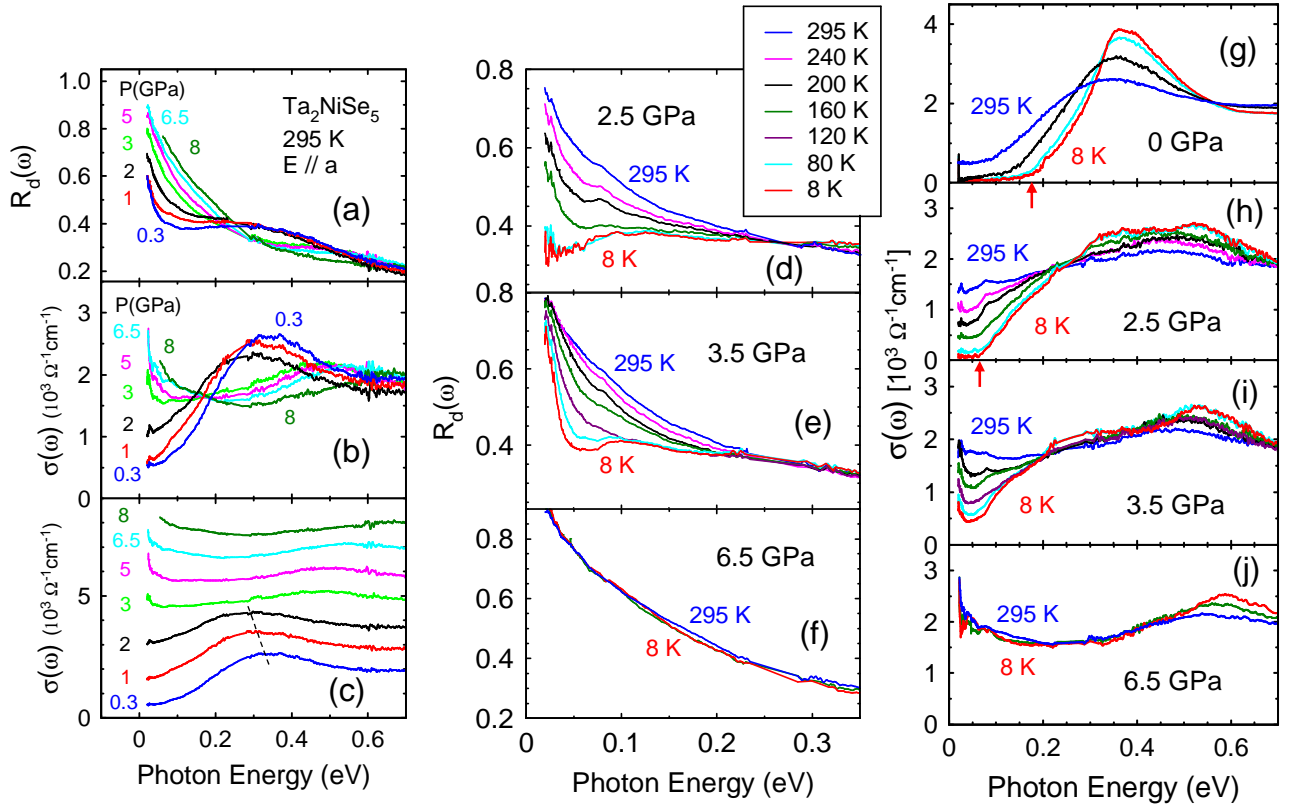


FIG. 4: (a) Optical reflectance [$R_d(\omega)$] and (b)(c) conductivity [$\sigma(\omega)$] of Ta_2NiSe_5 at 295 K under high pressure (P). $R_d(\omega)$ in the 0.235-0.285 eV range has been interpolated by a straight line since it could not be measured well due to strong absorption by diamond.⁴¹ In (c), the same spectra as those in (b) are vertically offset, and the broken line indicates the shift and suppression of the excitonic peak. (d)-(f) $R_d(\omega)$ of Ta_2NiSe_5 measured at $P=2.5, 3.5,$ and 6.5 GPa and at different temperatures. (g)-(j) $\sigma(\omega)$ of Ta_2NiSe_5 at $P=0, 2.5, 3.5,$ and 6.5 GPa and at low temperatures. The red vertical arrows indicate the onset of $\sigma(\omega)$ discussed in the text. The same temperature labels (the colors of the curves) apply in (d)-(f) and (g)-(j).

at around 3 GPa is almost coincident with the structural transition at P_s (Fig. 2). Since P_s is believed to be the boundary of EI phase,²³ it is reasonable that the excitonic peak is suppressed above P_s . The broadening and red shift of the excitonic peak below P_s probably indicate the weakening of excitonic correlation even within the EI phase below P_s . As discussed in Appendix, Raman spectra of Ta_2NiSe_5 at high P were also measured, using the same DAC and sample condition. The Raman spectra (Fig. 7) exhibit a sudden shift and disappearance of phonon peaks around 3 GPa, which should result from the first order structural transition at P_s . This Raman result further supports that the observed spectral changes in $\sigma(\omega)$ indeed result from the structural transition at P_s . With increasing P above 3 GPa, $\sigma(\omega)$ further increases and shows metallic characteristics with a rising (Drude) component toward zero energy.

Temperature dependent $R_d(\omega)$ spectra at $P=2.5, 3.5$ and 6.5 GPa are indicated in Figs. 4(d)-(f), and the corresponding $\sigma(\omega)$ spectra in Figs. 4(h)-4(j). First, note that the large T dependences of $R_d(\omega)$ and $\sigma(\omega)$ observed at $P=0$ are progressively reduced with increasing P . Ac-

cordingly, both the energy gap and excitonic peak at low T are progressively suppressed with P . At 2.5 GPa, $\sigma(\omega)$ develops a clear energy gap with cooling [Fig. 4(h)], but the onset of $\sigma(\omega)$ at 8 K is located at 0.062 eV, which is much smaller than that at $P=0$ [Fig. 4(g)]. Namely, a clear energy gap still exists at $P=2.5$ GPa, but its width is significantly reduced from that at $P=0$. At 3.5 GPa, $\sigma(\omega)$ below 0.2 eV is still strongly reduced with cooling, but unlike those at $P=0$ and 2.5 GPa, it is not completely depleted even at 8 K. A rising component toward zero energy is observed 8 K, which should be a Drude component due to free carriers. The thermal energy $k_B T$, where k_B is the Boltzmann constant, is about 0.7 meV at 8 K, while the tail of the Drude component at 8 K extends to much higher energy, ~ 50 meV. Therefore, the electronic state at 3.5 GPa and 8 K is difficult to understand as a semiconductor with thermally excited free carriers. Instead, it should be a semimetal with a band overlap of the order of 50 meV. Accordingly, the energy gap at 3.5 GPa should be a partial one, which is open only in certain portions of the Brillouin zone.²³ At 6.5 GPa, the spectra show only minor T dependences, and $\sigma(\omega)$ below

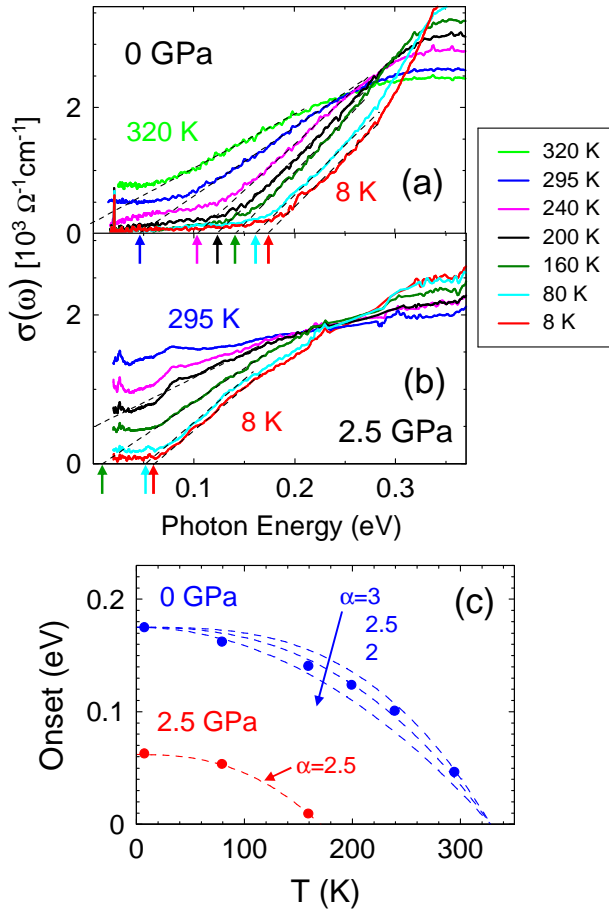


FIG. 5: Low-energy portion of $\sigma(\omega)$ in $E \parallel a$ polarization at (a) $P=0$ and (b) $P=2.5$ GPa. The broken lines indicate extrapolations to the linear-in-energy portion of the spectra, and the vertical arrows indicate the onset given by the zero crossing. (c) The onset energy in (a) and (b) plotted as a function of temperature (T). The broken curves indicate $\Delta(T) = \Delta(0)\{1 - (T/T_c)^\alpha\}$ with the indicated values of α . $\Delta(0)=0.175$ eV and $T_c=328$ K are used for $P=0$, and $\Delta(0)=0.062$ eV and $T_c=170$ K for $P=2.5$ GPa.

0.4 eV is almost unchanged from 295 to 8 K. Clearly, at 6.5 GPa there is no energy gap in Ta_2NiSe_5 and its electronic structure is quite metallic.

To examine more closely the variations of energy gap with P and T , the low-energy portion of $\sigma(\omega)$ at $P=0$ and 2.5 GPa are displayed in Figs. 5(a) and 5(b), respectively. The broken lines are extrapolations to the linear-in-energy portion in $\sigma(\omega)$. Their zero crossings, marked with the vertical arrows, indicate the onset of $\sigma(\omega)$. Here we regard the onset energy as the gap width Δ , following a previous $\sigma(\omega)$ work on Ta_2NiSe_5 (Ref. [22]) and other optical studies on strongly correlated electron systems.⁴⁷ At $P=0$ [Fig. 5(a)], the extrapolation crosses zero at 295 K and below, but not at 320 K. Namely, the gap in $\sigma(\omega)$ becomes fully open at 295 K and be-

low, which is reasonable since the gap formation starts below $T_c=328$ K and the gap is not well developed yet at 320 K. The T dependence of the onset energy is plotted in Fig. 5(c). The result is similar to that previously reported by Ref. [22], which reported a T dependence of the form $\Delta(T) = \Delta(0)\{1 - (T/T_c)^\alpha\}$ with $\alpha=2$. For comparison, in Fig. 5(c) we also plot this function with $T_c=328$ K and $\alpha=2, 2.5$, and 3. It is seen that the present data is close to $\alpha=2.5$, but cannot be well described by a single exponent. At 2.5 GPa [Fig. 5(b)], the extrapolation crosses zero at 160 K and below, but not at 200 K. Namely, the gap becomes fully open at 160 K and below, which is much lower than $T_c \simeq 290$ K at 2.5 GPa. This is in contrast to the $P=0$ case above, where the gap in $\sigma(\omega)$ is already open at 295 K which is below but still close to $T_c=328$ K. Namely, it seems that the P dependence of the energy gap in $\sigma(\omega)$ is different from that of T_c . The T dependence of the onset at 2.5 GPa is also plotted in Fig. 5(c). It is similar to that at $P=0$, but to fit with the form $\Delta(T) = \Delta(0)\{1 - (T/T_c)^\alpha\}$, $T_c \simeq 170$ K and $\alpha \simeq 2.5$ are required as shown by the broken curve in Fig. 5(c). Note that the use of this functional form is only phenomenological, and not based on a microscopic model for EI. The much stronger suppression of energy gap by pressure than that of T_c will be discussed again later.

To analyze the spectral weight (SW) transfer in $\sigma(\omega)$ with P and T , the effective electron number $N^*(\omega)$ per formula unit (fu) of Ta_2NiSe_5 , expressed as³⁹

$$N^*(\omega) = \frac{n}{m^*}(\omega) = \frac{2m_0}{\pi e^2 N_0} \int_0^\omega \sigma(\omega') d\omega', \quad (1)$$

is plotted in Fig. 6. Here, n , m^* and e are the electron density, effective mass in units of the rest mass m_0 , and the elementary charge. N_0 is the number of fu's per unit volume, which was calculated using the high P crystal structure data.^{34,48} $N^*(\omega)$ can be regarded as the number of electrons that contribute to $\sigma(\omega)$ between 0 and ω , therefore it directly reflects the SW transfer up to ω . At all P and T in Fig. 6, $N^*(\omega)$ at 1 eV is of the order of 1 fu⁻¹, which is reasonable compared with the total DOS within 1 eV from E_F given by band calculations.²³ At $P=0$, $N^*(\omega)$ varies with T over a wide energy range. The $N^*(\omega)$ spectra at different temperatures do not converge even at 1 eV, showing that the electronic structure reconstruction in the EI phase occurs over a wider energy scale than the gap width (0.17 eV) and the excitonic peak energy (0.4 eV). At 2.5 and 3.5 GPa, however, $N^*(\omega)$ varies with T only up to about 0.6 eV, indicating that the SW transfer is complete within 0.6 eV. At 6.5 GPa, $N^*(\omega)$ is almost independent of T . These results show that both the amount and energy range of the SW transfer are progressively suppressed by P , which is closely related with the suppression of energy gap.

As discussed in Introduction, it has been pointed out that the gap formation in Ta_2NiSe_5 below P_s may be partly due to e - l coupling, rather than being solely due to e - h (excitonic) correlation. If their relative contribu-

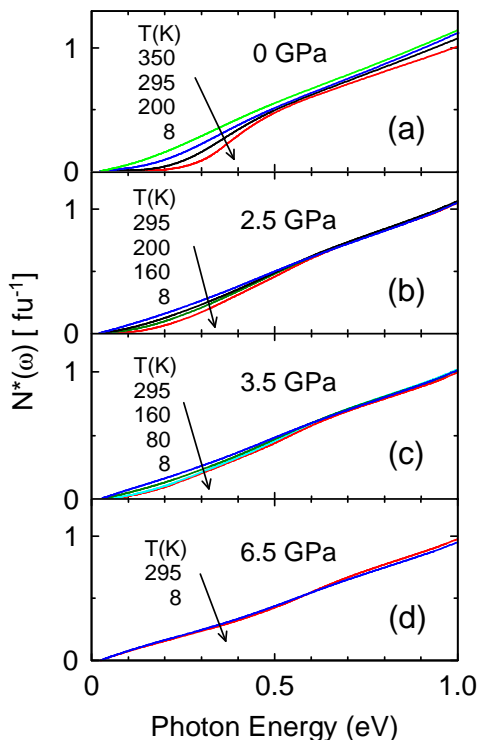


FIG. 6: Effective electron number $N^*(\omega)$ per formula unit (fu) of Ta_2NiSe_5 , calculated with Eq. (1) and the measured $\sigma(\omega)$ spectra at different pressures and temperatures.

tions do not change with P , and if both the structural transition at T_c and the gap opening below T_c are driven by a common mechanism, then one would naively expect that Δ and T_c should have similar P dependences. This is in contrast to the present results, in which the reduction of Δ by pressure is much greater than that of T_c (from $\Delta=0.17$ eV and $T_c=328$ K at $P=0$ to $\Delta=0.062$ eV and $T_c \simeq 290$ K at 2.5 GPa). Namely, in terms of the P dependence, Δ is not scaled with T_c . Interestingly, a pressure decoupling between electronic and structural transitions has been observed in BaFe_2As_2 ,⁴⁹ which is another pressure-induced superconductor. The present results for Ta_2NiSe_5 may suggest that, somehow, the e - h correlation is more responsible for the gap development below T_c , while the e - l coupling is more responsible for the structural transition at T_c . This would naturally lead to a stronger suppression of Δ than T_c by pressure, since the e - h correlation is likely more reduced by pressure than the e - l coupling as long as the structure does not change. An understanding of these P dependences based on a specific microscopic model is beyond the scope of the present study. It is hoped that effects of both the e - h correlation and the e - l coupling with symmetry breaking-

induced hybridization are both included in a microscopic model to understand the pressure evolution of electronic states in Ta_2NiSe_5 .

IV. SUMMARY

$\sigma(\omega)$ spectra of Ta_2NiSe_5 , a strong candidate for an EI, have been measured at high pressures and at low temperatures. A clear energy gap of about 0.17 eV and a marked excitonic peak at 0.38 eV at $P=0$ are suppressed with increasing P , which is especially marked across the structural transition at $P_s=3$ GPa. At 2.5 GPa ($< P_s$), the gap is still clearly open with a reduced width of 0.062 eV, but at 3.5 GPa ($> P_s$), the gap is partially filled, indicating that the ground state above P_s is semimetallic. At 6.5 GPa, $\sigma(\omega)$ shows very metallic characteristics with no energy gap. These results have been discussed in terms of a progressive weakening of excitonic correlation with pressure. Also, it is noted that the reduction of energy gap with pressure is much greater than that of T_c . This result may suggest that the relative importance of e - h correlation and e - l coupling in the gap formation changes with pressure.

ACKNOWLEDGMENTS

We would like to thank Prof. K. Matsubayashi, Prof. Y. Ohta, and Prof. K. Sugimoto for useful discussions. Experiments at SPring-8 were performed under the approval by JASRI (Proposal numbers 2013A1085, 2015B1698, 2016A1166, 2017A1163, 2017A1164.) This work was supported by KAKENHI (21102512, 23540409, 26400358, 19H00659, 17H06456)

Appendix: Raman spectra at high pressures

Raman scattering spectra of Ta_2NiSe_5 measured at high pressures and at 295 K are shown in Fig. 7. The measurement was made under a back scattering geometry on an as-grown sample surface containing the ac plane. A standard micro-Raman apparatus was used with a 532 nm laser source polarized along the a axis. High pressures were applied using the same DAC as that used for the $\sigma(\omega)$ studies, with exactly the same procedure for sample loading. In Fig. 7, the Raman peaks are due to optical phonons.²⁴⁻²⁶ As indicated by the broken lines in Fig. 7, the peak near 100 cm^{-1} is blue shifted and the peak near 125 cm^{-1} disappears in the spectra at 3.1 GPa and above. These sudden changes should result from the first-order structural phase transition at P_s (Fig. 2), where the rippling of the ac plane along c axis is reduced above P_s .^{23,34}

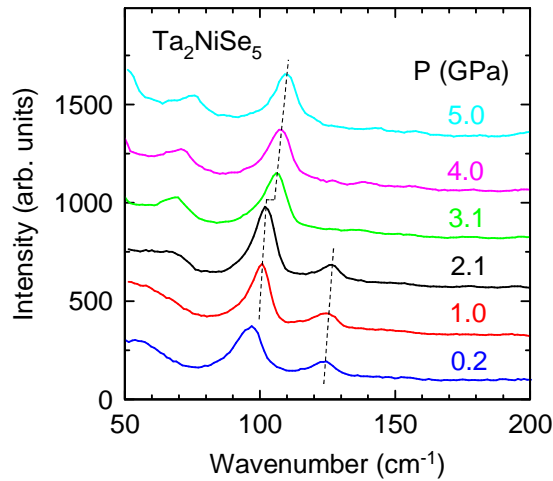


FIG. 7: Raman spectra of Ta_2NiSe_5 measured at high pressures (P) and at 295 K. The spectra are vertically offset for clarity. The excitation was made at 532 nm with $E \parallel a$ polarization. The broken lines are guide to the eye, emphasizing the sudden changes at around 3 GPa.

- * Electronic address: ho@tokushima-u.ac.jp
- ¹ For review on the early development, see, for example, B. I. Halperin and T. M. Rice, *Rev. Mod. Phys.* **40**, 755 (1968).
 - ² B. Bucher, P. Steriner, and P. Wachter, *Phys. Rev. Lett.* **67**, 2717 (1991).
 - ³ H. Cercellier, C. Monney, F. Clerc, C. Battaglia, L. Despont, M. G. Garnier, H. Beck, P. Aebi, L. Patthey, H. Berger, and L. Forro, *Phys. Rev. Lett.* **99**, 146403 (2007).
 - ⁴ Y. Wakisaka, T. Sudayama, K. Takubo, T. Mizokawa, M. Arita, H. Namatame, M. Taniguchi, N. Katayama, M. Nohara and H. Takagi, *Phys. Rev. Lett.* **103**, 026402 (2009).
 - ⁵ S. Sunshine and J. Ibers, *Inorg. Chem.* **24**, 3611 (1985).
 - ⁶ F. Di Salvo, C. Chen, R. Fleming, J. waszczak, R. Dun, S. Sunshine and J. Ibers, *J. Less-Common Met.* **116**, 51 (1986).
 - ⁷ K. Seki, Y. Wakisaka, T. Kaneko, T. Toriyama, T. Konishi, T. Sudayama, N. L. Saini, M. Arita, H. Namatame, M. Taniguchi, N. Katayama, M. Nohara, H. Takagi, T. Mizokawa, and Y. Ohta *Phys. Rev. B* **90**, 155116 (2014).
 - ⁸ T. Kaneko, T. Toriyama, T. Konishi, and Y. Ohta, *Phys. Rev. B* **87**, 035121 (2013).
 - ⁹ Y. F. Lu, H. Kono, T. I. larkin, A. W. Rost, T. Takayama, A. V. Boris, B. Keimer, and H. Takagi, *Nat. Commun.* **8**, 14408 (2017).
 - ¹⁰ T. I. Larkin, A. N. Yaresko, D. Propper, K. A. Kikoin, Y. F. Lu, T. Takayama, Y.-L. Mathis, A. W. Rost, H. Takagi, B. keimer and A. V. Boris, *Phys. Rev. B* **95**, 195144 (2017).
 - ¹¹ K. Sugimoto, S. Nishimot, T. Kaneko, and Y. Ohta, *Phys. Rev. Lett.* **120** (2018), 247602.
 - ¹² S. Mor, M. Herzog, D. Golez, P. Werner, M. Eckstein, N. Katayama, M. Nohara, H. Takagi, T. Mizokawa, C. Monney, and J. Stähler, *Phys. Rev. Lett.* **119**, 086401 (2017).
 - ¹³ K. Okazaki, Y. Ogawa, T. Suzuki, T. Yamamoto, T. Someya, S. Michimae, M. Watanabe, Y. Lu, M. Nohara, H. Takagi, N. Katayama, H. Sawa, M. Fujisawa, T. Kanai, N. Ishii, J. Itatani, T. Mizokawa, and S. Shin, *Nat. Commun.* **9**, 4322 (2018).
 - ¹⁴ T. Mitsuoka, T. Suzuki, H. Takagi, N. Katayama, H. Sawa, M. Nohara, M. Watanabe, J. Xu, Q. Ren, M. Fujisawa, T. Kanai, J. Itatani, S. Shin, K. Okazaki, and T. Mizokawa, *J. Phys. Soc. Jpn.* **89**, 124703 (2020).
 - ¹⁵ T. Tang, H. Wang, S. Duan, Y. Yang, C. Huang, Y. Guo, D. Qian, and W. Zhang *Phys. Rev. B* **101**, 235148 (2020).
 - ¹⁶ T. Suzuki, Y. Shinohara, Y. Lu, M. Watanabe, J. Xu, K. Ishikawa, H. Takagi, M. Nohara, N. Katayama, H. Sawa, M. Fujisawa, T. Kanai, J. Itatani, T. Mizokawa, S. Shin, and K. Okazaki, *Phys. Rev. B* **103**, L121105 (2021).
 - ¹⁷ T. Saha, D. Golez, G. De Ninno, J. Mravlje, Y. Murakami, B. Ressel, M. Stupar, and P. R. Ribic, *Phys. Rev. B* **103**, 144304 (2021).
 - ¹⁸ K. Fukutani, R. Stania, J. Jung, E. F. Schwier, K. Shimada, C. I. Kwon, J. S. Kim, and H. W. Yeom, *Phys. Rev. Lett.* **123**, 206401 (2019).
 - ¹⁹ L. Chen, T. T. Han, C. Cai, Z. G. Wang, Y. D. Wang, Z. M. Xin, and Y. Zhang, *Phys. Rev. B* **102**, 161116(R) (2020).
 - ²⁰ M. D. Watson, I. Markovic, E. A. Morales, P. Le Fevre, M. Merz, A. A. Haghighirad, and P. D. C. King, *Phys. Rev. Res.* **2**, 013236 (2020).
 - ²¹ K. Fukutani, R. Stania, C. I. Kwon, J. S. Kim, K. J. Kong, J. Kim, and H. W. Yeom, *Nat. Phys.* **17**, 1024 (2021).
 - ²² Y.-S. Seo, M. J. Eom, J. S. Kim, C.-J. Kang, B. I. Min, and J. Hwang, *Sci. Refp.* **8**, 11961 (2018).
 - ²³ K. Matsubayashi, H. Okamura, T. Mizokawa, N. Katayama, A. Nakano, H. Sawa, T. Kaneko, T. Toriyama,

- T. Konishi, Y. Ohta, H. Arima, R. Yamanaka, A. Hisada, T. Okada, Y. Ikemoto, T. Moriwaki, K. Munakata, A. Nakao, M. Nohara, Y. Lu, H. Takagi, and Y. Uwatoko, *J. Phys. Soc. Jpn.* **90**, 074706 (2021).
- ²⁴ J. Yan, R. Xiao, X. Luo, H. Lv, R. Zhang, Y. Sun, P. Tong, W. Lu, W. Song, X. Zhu, and Y. Sun, *Inorg. Chem.* **58**, 9036 (2019).
- ²⁵ M.-J. Kim, A. Schulz, T. Takayama, M. Isobe, H. Takagi, and S. Kaiser, *Phys. Rev. Res.* **2**, 042039(R) (2020).
- ²⁶ S. Pal, S. Grover, L. Harnagea, P. Telang, A. Singh, D. V. S. Muthu, U. V. Waghmare, and A. K. Sood, *Phys. Rev. Res.* **2**, 043182 (2020).
- ²⁷ K. Kim, H. Kim, J. Kim, C. Kwon, J. S. Kim, and B. J. Kim, *Nat. Commun.* **12**:1969 (2021).
- ²⁸ P. A. Volkov, M. Ye, H. Hohani, I. Feldman, A. Kanigel, and G. Blumberg, *npj Quantum Materials*, **6**:52 (2021),
- ²⁹ D. Werdehausen, T. Takayama, M. Höppner, G. Albrecht, A. W. Rost, Y. Lu, D. Manske, H. Takagi, and S. Kaiser, *Sci. Adv.* **4**:eaap8652 (2018).
- ³⁰ S. Mor, M. Herzog, J. Noack, N. Katayama, M. Nohara, H. Takagi, A. Trunschke, T. Mizokawa, C. Monney, and J. Sähler, *Phys. Rev. B* **97**, 115154 (2018).
- ³¹ T. Miyamoto, M. Mizui, N. Takamura, J. Hirata, H. Yamakawa, T. Morimoto, T. Terashige, N. Kida, A. Nakano, H. Sawa, and H. Okamoto, *J. Phys. Soc. Jpn.* **91**, 023701 (2022).
- ³² C. Monney, M. Herzog, A. Pulkkinen, Y. Huang, J. Pelli-ciari, P. Olade-Velasco, N. Katayama, M. Nohara, H. Takagi, T. Schmitt, and T. Mizokawa, *Phys. Rev. B* **102**, 085148 (2020).
- ³³ H. Lu, M. Rossi, J.-H. Kim, H. Yavas, A. Said, A. Nag, M. Garcia-Fernandez, S. Agrestini, K.-J. Zhou, C. Jia, B. Moritz, T. P. Devereaux, Z.-X. Shen, and W.-S. Lee, *Phys. Rev. B* **103**, 235159 (2021).
- ³⁴ A. Nakano, K. Sugawara, S. Tamura N. Katayama, K. Matsubayashi, T. Okada, Y. Uwatoko, K. Munakata, A. Nakao, H. Sagayama, R. Kumai, K. Sugimoto, N. Maejima, A. Machida, T. Watanuki, and H. Sawa, *IUCrJ* **5**, 158 (2018).
- ³⁵ J. Lee, C.-J. Kang, M. J. Eom, J. S. Kim, B. I. Min, and H. W. Yeom, *Phys. Rev. B* **99**, 075408 (2019).
- ³⁶ A. Subedi, *Phys. Rev. Mater.* **4**, 083601 (2020).
- ³⁷ G. Mazza, M. Rösner, L. Windgätter, S. Latini, H. Hübener, A. J. Millis, A. Rubio, and A. Georges, *Phys. Rev. Lett.* **124**, 197601 (2020).
- ³⁸ H. Okamura, Chapter 4 in *Optical Techniques for Solid State Materials Characterization* (R. Prasankumar and A. Taylor, Ed.), CRC Press (2011).
- ³⁹ M. Dressel and G. Grüner, *Electrodynamics of Solids* (Cambridge University Press, Cambridge, 2002).
- ⁴⁰ Above the measured range, $R_0(\omega)$ was first extrapolated with a function of the form $\omega^{-0.7}$ up to 15 eV, then with ω^{-4} up to 35 eV. The choice of these functions is certainly arbitrary, but they were chosen so that the $\sigma(\omega)$ obtained with the KK analysis of the extrapolated $R_0(\omega)$ was consistent with the previously reported $\sigma(\omega)$ measured with the ellipsometry.¹⁰
- ⁴¹ H. Okamura, Y. Ikemoto, T. Mariwaki, and T. Nanba, *Jpn. J. Appl. Phys.* **56**, 05FA11 (2017).
- ⁴² G. J. Piermarini, S. Block, J. D. Barnett, and R. A. Forman, *J. Appl. Phys.* **46**, 2774 (1975).
- ⁴³ H. Okamura, *J. Phys.: Conf. Ser.* **359**, 012013 (2012).
- ⁴⁴ S. Kimura and H. Okamura, *J. Phys. Soc. Jpn.* **82**, 021004 (2013).
- ⁴⁵ T. Moriwaki and Y. Ikemoto, *Infrared Phys. Tech.* **51**, 400 (2008).
- ⁴⁶ The present data at $P=0$ have been measured on more recent and larger samples than those used in Ref. [23]. Although the present $R_0(\omega)$ spectra in the infrared range [Fig. 3(a)] are similar to those used in Ref. [23], the present $\sigma(\omega)$ spectra [Fig. 3(b)] are about 30 % higher and their onset at low T is much clearer than those in Ref. [23]. These differences have mainly resulted from a much higher $R_0(\omega)$ in the visible-UV range in the present data and the high-energy extrapolations used. Note that a change in $R_0(\omega)$ at a higher energy range may cause a change in $\sigma(\omega)$ at a lower energy range through the KK relation.³⁹
- ⁴⁷ D. N. Basov, R. D. Averitt, D. van der Marel, M. Dressel, and K. Haule, *Rev. Mod. Phys.* **83**, 471 (2011).
- ⁴⁸ The volume per fu at room temperature and $P=0$, 2.5, 3.5, and 6.5 GPa have been estimated to be 173, 165, 159, and 150 \AA^3 , respectively, from the crystal structure data at high P .³⁴ In the calculation of $N^*(\omega)$, the volume contraction with cooling has been neglected, since it is much smaller than that with increasing P .
- ⁴⁹ J. J. Wu, J.-F. Lin, X. C. Wang, Q. Q. Liu, J. L. Zhu, Y. M. Xiao, P. Chow, and C. Jin, *Proc. Natl. Acad. Sci.* **110**, 17263 (2013).